

Galactic cannibalism and CDM density profiles

C. Nipoti^{1*}, T. Treu^{2,3}, L. Ciotti⁴, and M. Stiavelli⁵

¹*Theoretical Physics, Oxford University, 1 Keble Road, Oxford OX1 3NP, UK*

²*Department of Physics & Astronomy, UCLA, Box 951547, Los Angeles, CA 90095-1547*

³*Hubble fellow*

⁴*Department of Astronomy, Bologna University, via Ranzani 1, 40127 Bologna, Italy*

⁵*Space Telescope Science Institute, 3700 San Martin Drive, Baltimore, MD 21218*

Accepted, 8th September 2004; in original form, 5th April 2004

ABSTRACT

Using N-body simulations we show that the process of formation of the brightest cluster galaxy through dissipationless galactic cannibalism can affect the inner cluster dark matter density profile. In particular, we use as realistic test case the dynamical evolution of the galaxy cluster C0337-2522 at redshift $z = 0.59$, hosting in its centre a group of five elliptical galaxies which are likely to be the progenitor of a central giant elliptical. After the formation of the brightest cluster galaxy, the inner cluster dark matter density profile is significantly flatter (logarithmic slope $0.49 \lesssim \beta \lesssim 0.90$) than the original cusp ($\beta = 1$), as a consequence of dynamical friction heating of the massive galaxies against the diffuse cluster dark matter. In our simulations we have assumed that the cluster galaxies are made of stars only. We also show that the presence of galactic dark matter haloes can steepen the cluster central density profile. We conclude that galactic cannibalism could be a viable physical mechanism to reconcile – at least at the cluster scale – the flat dark matter haloes inferred observationally in some galaxy clusters with the steep haloes predicted by cosmological simulations.

Key words:

dark matter – galaxies: elliptical and lenticular, cD – galaxies: clusters: general

1 INTRODUCTION

Cold Dark Matter (CDM) cosmological simulations predict that the inner density profile of dark matter (DM) haloes is characterized by a cusp: $\rho_{\text{DM}}(r) \propto r^{-\beta}$, with logarithmic slope $\beta \sim 1-1.5$ for $r \rightarrow 0$: the exact value of the slope and its universality are at the centre of a lively debate. For example, several authors (Navarro, Frenk & White 1996, NFW; Moore et al. 1998; Ghigna et al. 2000; Navarro et al. 2004) claim that the resulting profiles are universal, in the sense that β is independent of the halo mass, while other authors suggest that the inner profile depends significantly on the slope of the power spectrum, so that the higher is the mass of the halo the steeper is the cusp (Subramanian, Cen & Ostriker 2000; Ricotti 2003, and references therein).

These predictions have been extensively tested by observations both in galaxies (e.g., Salucci & Burkert 2000; van den Bosch et al. 2000; de Blok et al. 2001; Simon et al. 2003) and in clusters of galaxies (e.g., Smith et al. 2001; Sand, Treu & Ellis 2002; Kelson et al. 2002; Gavazzi et al. 2003; Lewis, Buote & Stocke 2003; Sand et al. 2004). The derived values of β range from ~ 0 to ~ 1.3 . The observational results – shallow slopes and intrinsic scatter – could represent a serious challenge to the standard cosmological model, and exotic

scenarios have been also proposed to solve this problem (e.g. Spergel & Steinhardt 2000).

In any case, the role of baryons must be better understood before we are forced to reject a successful paradigm. In fact, it is well known that on scales of the order of kiloparsecs baryons are important and their evolution may affect substantially the DM distribution (see Binney 2004 for a discussion). For example, in the so-called “adiabatic contraction” approximation (Blumenthal et al. 1986; Gnedin et al. 2004), baryon dissipation effectively steepens the inner density profile of the host halo (Mo, Mao & White 1998; Kochanek & White 2001), thus exacerbating the contrast between theory and observations.

Here, motivated by recent observational studies of galaxy clusters based on a joint lensing and dynamical analysis – in which Sand et al. (2002, 2004) report inner logarithmic slopes in the range¹ $\beta = 0.38 - 0.99$ – we focus on the cluster-sized DM haloes, which are considered to be less

¹ The uncertainties on β could be higher than those given by Sand et al. (2004) if the ellipticity of the cluster mass distribution is higher than estimated by the authors (cf. Dalal & Keeton 2004; Bartelmann & Meneghetti 2004). Additional observational work is currently under way to clarify those issues and measure the distribution of DM inner slopes for larger samples of clusters.

* E-mail: nipoti@thphys.ox.ac.uk

affected by baryon dissipation, with respect to galaxy-sized haloes.

We note that the spiraling in of massive galaxies in clusters could flatten the cluster DM distribution, by heating it through dynamical friction (similar to the galaxy-globular cluster interaction at smaller scales; see Bertin, Liseikina & Pegoraro 2003). Recently, El-Zant et al. (2004), using N-body simulations, found that dynamical friction heating due to galaxies, modeled as rigid baryons clumps, is indeed effective in flattening the inner DM profile in clusters. Similar conclusions, in a different context, were also reached by Ma & Boylan-Kolchin (2004), who explored with N-body simulations the effects of the dynamical evolution of (deformable) DM sub-haloes on the DM distribution of their host halo. On the other hand, the mass infall associated with the spiraling in of the galaxies towards the cluster centre deepens the central potential well. This dissipationless contraction, in contrast with dynamical friction heating, can result in shrinking the cluster DM distribution and steepening its inner density profile (see, e.g., Barnes & White 1984; Jesseit, Naab & Burkert 2002): the final density profile will be the result of the two competing effects (see also Section 4).

Here we investigate the effects of dynamical friction on the cluster DM distribution in a realistic scenario, by simulating the time evolution of the galaxy cluster C0337-2522 at redshift $z = 0.59$ (ROSAT Deep Cluster Survey; Rosati et al. 1998). This cluster is characterized by the presence of five bright elliptical galaxies (Es) located within ~ 30 kpc from the centre, in projection. Nipoti et al. (2003b, hereafter N03), using N-body simulations, showed that the five galaxies are very likely to merge and form a brightest cluster galaxy (BCG) by $z = 0$, in accordance with the predictions of the galactic cannibalism scenario (Ostriker & Tremaine 1975; see also Merritt 1983; Dubinski 1998). In the present work we consider the evolution of the underlying cluster DM distribution, with the aid of additional higher resolution simulations (see also Nipoti et al. 2003c). In our models the single galaxies, as well as the cluster DM, are represented by N-body distributions: this is particularly important, because tidal stripping could remove mass from the individual galaxies, thus altering the infall process and its effects on the cluster DM halo.

2 NUMERICAL SIMULATIONS

2.1 Initial conditions

Our simulations represent possible realizations of the dynamical evolution of C0337-2522 – a poor galaxy cluster, with five bright Es in its centre – from redshift $z = 0.59$ to the present. The observational data and the set up of the initial conditions are described in detail in N03.

In the initial conditions of the simulations the cluster is represented as a live spherically symmetric DM distribution, hosting five identical massive galaxies modeled as spherical N-body systems. For simplicity, we only consider simulations where each galaxy is represented by a single collisionless component (stars). This is justified under the assumption that the mass of the galaxies in the cluster centre is dominated by luminous matter (e.g. Treu & Koopmans 2004), and that the extended DM halo is likely to be tidally stripped in the innermost region of the cluster (e.g. Natarajan, Kneib & Smail 2002).

Table 1. Parameters of the simulations.

#	r_{cl}	M_{cl}	N_{DM}	N_{lum}	$r_{\text{DM},f}/r_{\text{cl}}$	β
1	100	4.8	235520	10240	$0.77^{+0.04}_{-0.04}$	$0.50^{+0.09}_{-0.09}$
1s	100	4.8	222720	23040	$0.75^{+0.04}_{-0.04}$	$0.49^{+0.07}_{-0.07}$
3	100	5.3	130560	5120	$0.91^{+0.03}_{-0.03}$	$0.89^{+0.04}_{-0.04}$
5a	100	9.6	120320	2560	$0.79^{+0.04}_{-0.04}$	$0.59^{+0.08}_{-0.08}$
6	100	9.6	120320	2560	$0.77^{+0.04}_{-0.04}$	$0.52^{+0.08}_{-0.07}$
7	100	10.6	266240	5120	$0.83^{+0.04}_{-0.04}$	$0.68^{+0.06}_{-0.06}$
14a	300	13.5	170240	2560	$0.93^{+0.03}_{-0.03}$	$0.90^{+0.06}_{-0.05}$
17	300	15.3	193280	2560	$0.84^{+0.05}_{-0.04}$	$0.72^{+0.08}_{-0.08}$
18	300	27.0	171520	1280	$0.91^{+0.03}_{-0.03}$	$0.86^{+0.05}_{-0.05}$
19	300	27.0	171520	1280	$0.86^{+0.05}_{-0.04}$	$0.76^{+0.08}_{-0.08}$
20	300	30.6	194560	1280	$0.89^{+0.05}_{-0.05}$	$0.81^{+0.06}_{-0.06}$
21	300	30.6	194560	1280	$0.91^{+0.03}_{-0.03}$	$0.85^{+0.05}_{-0.05}$
1.1	100	4.8	942080	40960	$0.76^{+0.04}_{-0.04}$	$0.51^{+0.08}_{-0.08}$
1s.1	100	4.8	890880	92160	$0.74^{+0.04}_{-0.04}$	$0.49^{+0.09}_{-0.09}$
3.1	100	5.3	1044480	40960	$0.90^{+0.05}_{-0.05}$	$0.89^{+0.08}_{-0.08}$
17.1	300	15.3	773120	10240	$0.84^{+0.04}_{-0.04}$	$0.72^{+0.08}_{-0.09}$
20.1	300	30.6	1556480	10240	$0.90^{+0.05}_{-0.05}$	$0.83^{+0.06}_{-0.07}$

First column: name of the simulation. r_{cl} : initial cluster break radius (kpc). M_{cl} : cluster mass ($10^{13} M_{\odot}$). N_{DM} : total number of DM particles. N_{lum} : total number of stellar particles. $r_{\text{DM},f}/r_{\text{cl}}$: best-fitting break radius of the final DM profile normalized to the initial break radius. β : best-fitting logarithmic slope of the final DM profile. 1σ uncertainties on $r_{\text{DM},f}/r_{\text{cl}}$ and β are reported. Simulations 1.1, 1s.1, 3.1, 17.1, and 20.1 are higher-resolution replicas of simulations 1, 1s, 3, 17, and 20, respectively. Pairs of runs with the same cluster parameters (5a and 6, 18 and 19, 20 and 21) differ in the initial centre-of-mass positions and velocities of the galaxies. In simulations 1s and 1s.1 50 small galaxies are added.

2.2 Models

For the cluster DM distribution we use a Hernquist (1990) model

$$\rho_{\text{cl}}(r) = \frac{M_{\text{cl}} r_{\text{cl}}}{2\pi r (r_{\text{cl}} + r)^3}, \quad (1)$$

with M_{cl} and r_{cl} cluster total mass and break radius, respectively. Thus, $\rho_{\text{cl}}(r) \sim r^{-1}$ for $r \rightarrow 0$, as in the NFW density profile, but, unlike the NFW profile, the total mass is finite, because $\rho_{\text{cl}}(r) \sim r^{-4}$ for $r \rightarrow \infty$. In the simulations the distribution function of the cluster has been chosen isotropic or radially anisotropic (see N03); r_{cl} is either 100 kpc or 300 kpc, and the total cluster mass is in the range $4.8 \times 10^{13} - 3.06 \times 10^{14} M_{\odot}$ (see Table 1).

At the beginning of each simulation the five galaxies are identical (isotropic or radially anisotropic) Hernquist models: their stellar density distribution ρ_* is described by equation (1), with break radius $r_* \simeq 2.2$ kpc and total mass $M_* = 4 \times 10^{11} M_{\odot}$. The initial centre-of-mass positions and velocities of the five galaxies are chosen by extraction from the cluster distribution function, constrained by the observational data (see N03). Note that simulations with the same cluster parameters (namely, the pairs of simulations 5a and 6, 18 and 19, 20 and 21; see Table 1) differ in the initial centre-of-mass positions and velocities of the galaxies. In simulations 1s and 1s.1 we consider an additional population of 50 smaller galaxies (each modeled as a Hernquist model with $M_* = 5 \times 10^{10} M_{\odot}$ and $r_* \simeq 0.55$ kpc) distributed in phase-space according to the cluster distribution function (see Fig. 1).

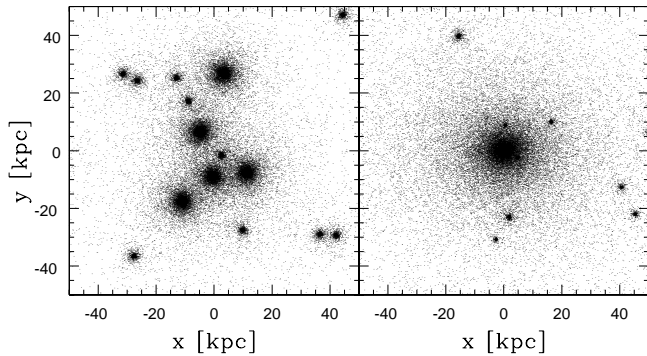


Figure 1. Simulation 1s.1: snapshots of the initial ($z = 0.59$, left) and final ($z = 0$, right) projected distribution of the stellar particles in the inner cluster region.

The total time of each simulation is ~ 6.1 Gyr, of the order of $100 T_{\text{dyn}}$, where T_{dyn} is the half-mass dynamical time of the initial galaxy models (we adopt $\Omega_m = 0.3$, $\Omega_\Lambda = 0.7$, and $H_0 = 65 \text{ km s}^{-1} \text{ Mpc}^{-1}$).

2.3 Codes and numerical tests

For most of the numerical N-body simulations (the first 12 listed in Table 1) we used the Springel, Yoshida & White (2001) GADGET code, with cell-opening parameter $\alpha = 0.02$, minimum and the maximum time step $\Delta t_{\text{min}} = 0$ and $\Delta t_{\text{max}} = T_{\text{dyn}}/100$, time step tolerance parameter $\alpha_{\text{tol}} = 0.05$, and softening parameter $\varepsilon \simeq 0.36 r_*$. Additional higher-resolution simulations (1.1, 1s.1, 3.1, 17.1, 20.1) were obtained using the parallel code FVFPS (Fortran Version of a Fast Poisson Solver; Londrillo, Nipoti & Ciotti 2003). This code, based on algorithms introduced by Dehnen (2002), has been successfully tested and compared with GADGET (Nipoti, Londrillo, Ciotti 2003a; Nipoti 2003). In particular, we adopted the following values of the parameters: minimum value of the opening parameter $\theta_{\text{min}} = 0.5$; softening parameter $\varepsilon \simeq 0.1 r_*$; initial time step $\Delta t \sim T_{\text{dyn}}/100$. In all simulations stellar and DM particles have the same mass, and the total energy is conserved within 1%.

Discreteness, two-body relaxation and softening are expected to artificially alter the very inner DM density profile. To quantify numerical effects, we ran a few test simulations where the initial conditions are represented by the cluster DM halo only, for the adopted codes and values of the parameters (softening, number of DM particles, time step, opening parameter, total elapsed time). The final profile of one of these test simulations (with the same parameters as simulation 1.1) is shown in Fig. 2 (empty symbols). In all the test simulations the Hernquist profile is preserved for $r \gtrsim 0.05 r_{\text{cl}}$. Thus, we only consider the properties of the cluster DM halo for $r \gtrsim 0.05 r_{\text{cl}}$ in the analysis of all the presented simulations. We note that in the initial conditions of the lowest-resolution of our simulations $r \sim 0.05 r_{\text{cl}}$ contains ~ 270 particles. Thus, our choice of the minimum reliable radius is consistent with recent numerical convergence studies (Power et al. 2003, and references therein).

Other possible numerical artifacts might be due to the small number of particles used to represent each galaxy (128 to 2048, in the simulations run with GADGET). In particular, it is likely that in our simulations we overestimate the galaxy mass that is tidally stripped (see Kazantzidis et al. 2004) and this might affect the response of the cluster DM.

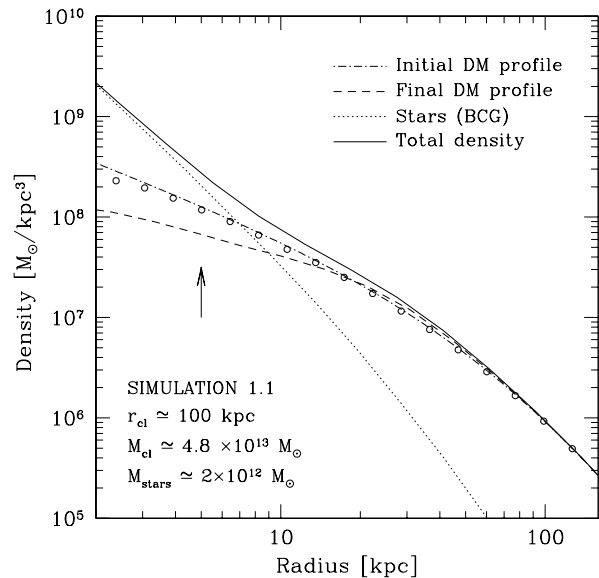


Figure 2. Final density distribution of the cluster dark, luminous and total matter in simulation 1.1. The dot-dashed curve is the initial (Hernquist) DM profile. The arrow indicates the minimum radius considered for the fit. Empty symbols refer to a test simulation run to exclude numerical artifacts (see Section 2.3).

To explore this problem we ran simulations 1.1, 1s.1, 3.1, 17.1, and 20.1, which have the same initial conditions as simulations 1, 1s, 3, 17, and 20, respectively, but higher total number of particles ($\sim 10^6$ DM particles, and 2048 to 8192 stellar particles for each of the five galaxies). We checked that all the relevant properties of the system evolve in the same way in the corresponding higher and lower resolution simulations. In particular the final cluster DM profile is practically indistinguishable in the two cases over the considered radial range $r \gtrsim 0.05 r_{\text{cl}}$.

3 RESULTS

In all the simulations 3 to 5 out of the 5 massive galaxies merge before $z = 0$ at the bottom of the cluster potential well, as a consequence of dynamical friction. Fig. 1 shows, as an example, the initial ($z = 0.59$, left) and final ($z = 0$, right) projected distributions of the *stellar* particles in the inner ~ 50 kpc for simulation 1s.1. In any case, the merger remnant is similar in its main structural and dynamical properties to a real BCG (see N03). Here we discuss the effects of this dissipationless multiple merging event on the underlying cluster DM distribution.

3.1 Properties of the final dark matter density profile

To quantify the combined effects of dynamical friction heating and dissipationless contraction, we fit the final angle-averaged DM density profile using a generalization of the Hernquist profile, in the form (Dehnen 1993)

$$\rho_{\text{DM}}(r) = \frac{\rho_{\text{DM},0} r_{\text{DM}}^4}{r^\beta (r_{\text{DM}} + r)^{4-\beta}}, \quad (2)$$

where the inner slope β and the break radius r_{DM} are free parameters, and the reference density $\rho_{\text{DM},0}$ is constrained

by the total DM mass. The initial cluster DM density profile (equation 1) corresponds to the case $\beta = 1$, $r_{\text{DM}} = r_{\text{cl}}$, and $\rho_{\text{DM},0} = M_{\text{cl}}/(2\pi r_{\text{cl}}^3)$. When computing the angle-averaged density profile of the final DM distribution, we determine the centre of the cluster using the iterative technique described by Power et al. (2003): the centre of mass of the system is computed recursively, considering particles within a sphere whose radius shrinks by 2.5 per cent at each step. We stop the iteration when the sphere contains ~ 1000 particles². The best-fitting β and r_{DM} for the final cluster DM distribution of each simulation are reported in Table 1; 1σ uncertainties on the best-fitting parameters are calculated from $\Delta\chi^2 = 2.30$ contours in the space $\beta - r_{\text{DM}}$.

Fig. 2 shows the final dark, luminous and total matter distribution for simulation 1.1: the final cluster DM distribution (dashed line) is centrally shallower than the initial Hernquist profile (dot-dashed line). The modification is apparent at $r \lesssim 20$ kpc, where the contribution of the newly formed central galaxy (dotted line) to the total density (solid line) becomes relevant. Thus, *the central cluster DM cusp after the formation of the BCG is flatter than the original $\rho_{\text{DM}} \propto r^{-1}$.*

We find the same qualitative behaviour of the final luminous and dark matter distributions in all the other simulations, though simulation 1.1 represents one of the cases where flattening is more effective (the final best-fitting β is ~ 0.5). Considering all of our simulations, we find best-fitting logarithmic slope β in the range $0.49 \lesssim \beta \lesssim 0.90$, with average $\langle\beta\rangle = 0.71$. Comparing the best-fitting final break radius $r_{\text{DM},f}$ with the break radius r_{cl} of the corresponding initial Hernquist model, we find $0.74 \lesssim r_{\text{DM},f}/r_{\text{cl}} \lesssim 0.95$, with average $\langle r_{\text{DM},f}/r_{\text{cl}} \rangle = 0.85$. We note that the *best-fitting* final break radius is not a direct measure of the concentration of the system, because it can be significantly affected by the change in the shape of the density distribution. In fact, the final radii containing 10, 50, 70 and 90 per cent of the total DM mass are always larger than 95 per cent of the corresponding initial values, even for quite small $r_{\text{DM},f}/r_{\text{cl}}$ (e.g., simulations 1 and 1s). Thus, in our models, deviations of $r_{\text{DM},f}$ from r_{cl} indicate a difference in the shape of the profile, as well as the value of β does.

Simulation 1s.1 has the same initial conditions (cluster mass, radius and distribution function, and phase space coordinates of the centres of mass of the galaxies) as simulation 1.1, but in the first case 50 smaller galaxies are added to the five massive galaxies to represent the cluster population (see Fig. 1). We find that the main properties of the final matter distribution in simulation 1s.1 are not significantly different from those of simulation 1.1. We conclude that even a rather simple model, representing only the more massive galaxies in the initial conditions, is sufficient to capture the main physical processes.

Thus, in the considered scenario we find that the most important effect of the formation of a BCG through galactic cannibalism on the underlying diffuse DM distribution is to produce a shallower final cluster DM distribution. In other words, dynamical friction heating is more effective than contraction due to the mass infall.

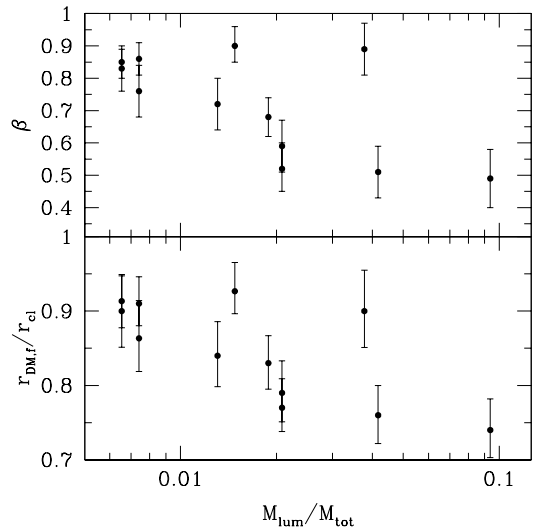


Figure 3. Best-fitting logarithmic inner slope β (top) and break radius $r_{\text{DM},f}$ (normalized to the initial break radius; bottom) of the final DM density distribution versus the ratio between the total mass in stars and total cluster mass (DM plus stars). Bars indicate 1σ uncertainties.

3.2 Physical interpretation

In Fig. 3 we plot the final best-fitting β (top) and $r_{\text{DM},f}/r_{\text{cl}}$ (bottom) as a function of the ratio $M_{\text{lum}}/M_{\text{cl}}$ between the total mass in stars and the total cluster mass (DM plus stars). The general trend is that the final density profile is shallower when $M_{\text{lum}}/M_{\text{cl}}$ is higher. However, the distribution of points in the plane $M_{\text{lum}}/M_{\text{cl}} - \beta$ (as well as in the plane $M_{\text{lum}}/M_{\text{cl}} - r_{\text{DM},f}/r_{\text{cl}}$) is characterized by a significant scatter: for example, simulations 1 and 3 have roughly the same $M_{\text{lum}}/M_{\text{cl}} \sim 0.04$, but significantly different final inner slopes ($\beta \sim 0.5$ and $\beta \sim 0.9$, respectively). This suggests that the cluster mass is not a discriminant in determining the final density profile. We argue that the orbital properties of the five galaxies represent the main factor affecting the final slope of the DM cusp. This picture would be consistent with our findings, because simulations with the same or similar $M_{\text{lum}}/M_{\text{cl}}$ (and cluster break radius) differ only in the initial phase-space coordinates of the galaxies in the cluster. In general, galaxies on different orbits will heat the underlying DM at different radii and at different rates. Thus, it is not surprising to find a range of values of β in simulations with similar cluster parameters, but different initial positions and velocities of the galaxies.

In order to quantify this effect, we present here the results of a very simple exercise. We ran two additional test simulations, with the same number of particles, cluster parameters and initial positions of the five galaxies as simulation 1, but different initial velocities. In one case each galaxy starts with half the initial kinetic energy it has in simulation 1 (and the same direction of the velocity vector), in the other the galaxies have null initial velocities. Interestingly, we find best-fitting final slopes $\beta \simeq 0.68$ in the former case, and $\beta \simeq 1.29$ in the latter, to be compared with $\beta \simeq 0.50$ for simulation 1. In other words, for fixed initial position of

² As a check, we also computed the centre of the system as the position of the lowest-potential energy particle, finding good agreement with the adopted method.

a galaxy, the smaller is its initial kinetic energy, the smaller the amount of energy it transfers to the cluster DM through dynamical friction heating. We also recall that the infall of the galaxies into the cluster centre deepens the cluster gravitational potential well. If the amount of dynamical friction heating is quite small (as in the extreme case of the test simulation in which the galaxies start at rest), then dissipationless contraction dominates and the final cusp is steeper than the initial.

We conclude that the orbital parameters of the galaxies are important in determining the final DM distribution, as clearly illustrated by the results of the two test simulations presented above. However, it must be stressed that these test simulations – intended only to isolate an important physical effect – are characterized by quite artificial initial conditions, which are not extracted from a distribution function and are not consistent with the observational phase-space constraints considered in our work (see N03).

3.3 Comparison with observations

How do the results of our simulations compare with observationally determined cluster DM density profiles? The galaxy clusters observed by Sand et al. (2004) are suitable for this kind of exercise. These clusters (MS2137-23, Abell 383, RXJ1133, Abell 963, MACS1206, Abell 1201) are at redshifts lower than that of C0337-2522, they have total mass of the order of a few $10^{14} M_{\odot}$, and they host a dominant giant elliptical (with mass around $10^{12} M_{\odot}$) apparently relaxed at the bottom of the cluster potential well. Sand et al. (2004) found slopes $0.38 \lesssim \beta \lesssim 0.99$ with an average value of $\langle \beta \rangle \sim 0.52$ for the first three clusters, and an upper limit $\beta < 0.57$ for the others. It appears that our simulations are able to reproduce their observations. In particular, it is very suggestive to compare the final matter distribution of simulation 1.1 with the best-fitting model that Sand et al. found for MS2137-23 (cf. Fig. 2 with their Fig. 7). The similarity of the DM and stellar distributions is striking: the best-fitting slope is $\beta = 0.57$ for MS2137-23 and $\beta = 0.50$ for the end-product of simulation 1.1. Not only can the proposed mechanism reconcile the shallow observed slopes with the steep slopes obtained in DM only simulations, but also the various realizations of the cannibalism process could introduce additional scatter, thus helping to explain the observed scatter.

Ultimately, when more observations are available and we can measure the *distribution* of the final slopes it might be possible to use the observed scatter to constrain the history of cannibalism in clusters.

4 SUMMARY AND CONCLUSIONS

In this paper we explored, with the aid of N-body simulations, the effects on the inner cluster DM density profile of the formation of a BCG, through dissipationless multiple merging of pre-existing galaxies. The initial conditions are designed to reproduce the observed galaxy cluster C0337-2522 ($z = 0.59$). Although we focus on a single well observed system as a case study, we stress that the results of the simulations could be generalized to poor galaxy clusters where the central giant elliptical was formed as a consequence of galactic cannibalism, with negligible dissipation.

We found that the inner cluster DM profile is sensitive to the dynamical evolution of cluster galaxies, and in particular

to the formation of a BCG. In our models, where the initial conditions are realistic and the galaxies are deformable, we find final slopes in the range $0.49 \lesssim \beta \lesssim 0.90$, with average $\langle \beta \rangle = 0.71$. The qualitative behaviour of our simulations is in agreement with what found by El-Zant et al. (2004), though they obtained a quite small value of the final inner slope ($\beta \simeq 0.35$), which is likely to be due to the use of rigid clumps, combined with a high fraction of luminous (clumped) matter ($M_{\text{lum}}/M_{\text{cl}} \simeq 0.06$). Dynamical friction heating in a cluster with original inner density profile $\rho_{\text{DM}} \propto r^{-1}$ can thus produce a flatter final inner slope for the cluster DM. Recent measures of the DM profiles of observed clusters can be interpreted taking into account this mechanism.

As outlined in the Introduction, our results are based on the assumption that cluster galaxies are essentially made of stars. However, in a scenario in which the contribution of galactic DM haloes to galaxy masses is important, the inspiraling galaxies might bring a significant amount of DM in the centre of the cluster. For instance, if we consider, as extreme case, that the massive galaxies in our simulations are made of DM only, the final DM cusp would be steeper than r^{-1} , because the DM infall is dominant over dynamical friction heating (cf. solid curve in Fig. 2). A similar scenario has been recently considered by Ma & Boylan-Kolchin (2004), who studied the interplay between a DM halo and its sub-haloes (see also Zhang et al. 2002). Ma & Boylan-Kolchin show with N-body simulations that the dynamical evolution of sub-haloes, depending on their mass and concentration, can either steepen or flatten the halo cusp. Thus, the determination of the amount and distribution of DM in cluster galaxies is very relevant also to the problem of the cluster cusp.

As a consequence, the discrepancies found between the observationally determined inner DM profiles and the predictions of CDM models must not necessarily represent a failure of CDM, at least at the cluster scale. Instead, they could reflect our poor understanding of the formation and evolution of galaxies, where the physics of baryons is important. These processes have to be taken into account when predicting the properties of DM haloes of clusters, on scales of few tens of kiloparsecs or smaller. At the same time, our simulations – when interpreted in the context of structure formation (i.e., galaxies considered as sub-haloes of DM) – indicate that is quite remarkable to obtain a universal DM profile as a result of successive aggregations³, due to the requirement that dynamical friction heating, potential well contraction, and mass increase all balance. This detailed balance should be further studied in cosmological simulations.

ACKNOWLEDGMENTS

We are grateful to Giuseppe Bertin, James Binney, Jeremiah Ostriker, David Sand, Graham P. Smith, and the anonymous referee for helpful comments on the draft. TT also acknowledges support from NASA through Hubble Fellowship grant HF-01167.01.

REFERENCES

Barnes J., White S.D.M., 1984, MNRAS, 211, 753

³ We note that a non-homology effect of successive dissipationless mergings was already reported by Nipoti et al. (2003a).

- Bartelmann M., Meneghetti M., 2004, *A&A*, 418, 413
- Bertin G., Liseikina T., Pegoraro F., 2003, *A&A*, 405, 73
- Binney J., 2004, *IAU Symposium 220*, “Dark Matter in Galaxies”, ed. S. Ryder, D.J. Pisano, M. Walker & K. Freeman, Publ. Astron. Soc. Pac, in press (astro-ph/0310219)
- Blumenthal G.R., Faber S.M., Flores R., Primack J.R., 1986, *ApJ*, 301, 27
- Dalal V., Keeton C.R., 2004, preprint (astro-ph/0312072)
- de Blok W.J.G., McGaugh S.S., Bosma A., Rubin V.C., 2001, *ApJ*, 552, L23
- Dehnen W., 1993, *MNRAS*, 265, 250
- Dehnen W., 2002, *Journal of Computational Physics*, 179, 27
- Dubinski J., 1998, *ApJ*, 502, 141
- El-Zant A., Hoffman Y., Primack J., Combes F., Shlosman I., 2004, *ApJ*, 607, L75
- Gavazzi R., Fort B., Mellier Y., Pellò R., Dantel-Fort M., 2003, *A&A*, 403, 11
- Ghigna S., Moore B., Governato F., Lake G., Quinn T., Stadel J., 2000, *ApJ*, 544, 616
- Gnedin O.Y., Kravtsov A.V., Klypin A.A., Nagai D., 2004, *ApJ*, submitted (astro-ph/0406247)
- Hernquist L., 1990, *ApJ*, 356, 359
- Jesseit R., Naab T., Burkert A., 2002, *ApJ*, 571, L89
- Kazantzidis S., Mayer L., Mastrogiuseppe C., Diemand J., Stadel J., Moore B., 2004, *ApJ*, 608, 663
- Kelson D.D., Zabludoff A.I., Williams K.A., Trager S.C., Mulchaey J.S., Bolte M., 2002, *ApJ*, 576, 720
- Kochanek C.S., White M., 2001, *ApJ*, 559, 531
- Lewis A.D., Buote D.A., Stocke J.T., 2003, *ApJ*, 586, 135
- Londrillo P., Nipoti C., Ciotti L., 2003, In “Computational astrophysics in Italy: methods and tools”, Roberto Capuzzo-Dolcetta ed., Mem. S.A.It. Supplement, vol. 1, p. 18
- Ma C.-P., Boylan-Kolchin M., 2004, *Phys. Rev. Lett.*, 93, 021301
- Merritt D., 1983, *ApJ*, 264, 24
- Mo H.J., Mao S., White S.D.M., 1998, *MNRAS*, 295, 319
- Moore B., Governato F., Quinn T., Stadel J., Lake G., 1998, *ApJ*, 499, L5
- Natarajan P., Kneib J.-P., Smail I., 2002, *ApJ*, 580, L11
- Navarro J.F., Frenk C.S., White S.D.M., 1996, *ApJ*, 462, 563 (NFW)
- Navarro J.F. et al., 2004, *MNRAS*, 349, 1039
- Nipoti C., 2003, PhD thesis, Univ. Bologna
- Nipoti C., Londrillo P., Ciotti L., 2003a, *MNRAS*, 342, 501
- Nipoti C., Stiavelli M., Ciotti L., Treu T., Rosati P., 2003b, *MNRAS*, 344, 748 (N03)
- Nipoti C., Stiavelli M., Ciotti L., Treu T., Rosati P., 2003c, preprint (astro-ph/0311424)
- Ostriker J.P., Tremaine S.D., 1975, *ApJ*, 202, L13
- Power C., Navarro J.F., Jenkins A., Frenk C.S., White S.D.M., Springel V., Stadel J., Quinn T., 2003, *MNRAS*, 338, 14
- Ricotti M., 2003, *MNRAS*, 344, 1237
- Rosati P., della Ceca R., Norman C., Giacconi R., 1998, *ApJ*, 492, L21
- Salucci P., Burkert A., 2000, *ApJ*, 537, L9
- Sand D.J., Treu T., Ellis R.S., 2002, *ApJ*, 574, L129
- Sand D.J., Treu T., Smith G.P., Ellis R.S., 2004, *ApJ*, 604, 88
- Simon J.D., Bolatto A.D., Leroy A., Blitz L., 2003, *ApJ*, 596, 957
- Smith G.P., Kneib J.-P., Ebeling H., Czoske O., Smail I., 2001, *ApJ*, 552, 493
- Spergel D.N., Steinhardt P.J., 2000, *Phys. Rev. Lett.*, 84, 3760
- Springel V., Yoshida N., White S.D.M., 2001, *New Astronomy*, 6, 79
- Subramanian K., Cen R., Ostriker J.P., 2000, *ApJ*, 538, 528
- Treu T., Koopmans L., 2004, *ApJ*, 611, 739
- van den Bosch F.C., Robertson B.E., Dalcanton J.J., de Blok W.J.G., 2000, *AJ*, 119, 1579
- Zhang B., Wyse R.F.G., Stiavelli M., Silk J., 2002, *MNRAS*, 332, 647

This paper has been typeset from a \TeX / \LaTeX file prepared by the author.